Contrib Mineral Petrol (1991) 109:98–113

Contributions to Mineralogy and Petrology
© Springer-Verlag 1991

Residence of trace elements in metasomatized spinel lherzolite xenoliths: a proton-microprobe study

Suzanne Y. O'Reilly[1], **W.L. Griffin**[2], **C.G. Ryan**[2]

[1] School of Earth Sciences, Macquarie University, Sydney, N.S.W. 2109, Australia
[2] Division of Exploration Geoscience, C.S.I.R.O., North Ryde, N.S.W. 2113, Australia

Abstract. Minerals occurring in dry and modally metasomatized spinel lherzolites from western Victoria have been analysed by proton microprobe for Ni, Cu, Zn, Ga, Rb, Sr, Y, Zr, Nb, Ba, Pb, Br, rare-earth elements (REE), Th and U. Mass-balance calculations demonstrate that these trace elements are contained in specific acceptor minerals and do not occur in significant concentrations at clean grain boundaries. The level of particular trace elements in the rock depends on the presence of specific phases: for example high levels of REE, Sr (and U, Th, Br) require apatite, while Ba, Nb and Ta are strongly concentrated in amphibole ± mica. Mantle metasomatism in these spinel lherzolites is inferred to result from an open-system process involving infiltration of fluids released by crystallizing silicate melts. This process produces metasomatic zones with different modal mineralogy and hence greatly different trace-element signatures. The data demonstrate that large-ion-lithophile (LIL) and high-field strength (HFS) elements in metasomatized spinel lherzolites are strongly concentrated in non-refractory phases, which will break down easily in heated volumes such as the walls of magma conduits. The heterogeneity observed in trace-element patterns of intraplate alkali basaltic rocks may not reflect source heterogeneity, but may result largely from contamination by metasomatized mantle wall rock. The K_Ds for most trace elements show little temperature dependence except for K_DSr between orthopyroxene and clinopyroxene where K_D decreases with increasing temperature. The generally uniform K_Ds can be used to test for disequilibrium in such assemblages.

Introduction

The subcontinental lithospheric mantle may be the source of some types of mafic magmas, and continental magmas of deeper origin must pass through it on their way to the surface. The chemical characteristics of this part of the lithosphere are therefore critical to understanding the geochemistry of mantle-derived continental magmas and the evolution of the crust/mantle system. To assess the geochemical characteristics of some continental lithospheric mantle domains, we have previously carried out a comprehensive study of a suite of spinel lherzolite xenoliths from western Victoria, in southeastern Australia (e.g. O'Reilly and Griffin 1988; Griffin et al. 1988).

The xenoliths studied are samples of a lithospheric mantle domain showing varying degrees of cryptic and modal metasomatism (as defined in Dawson 1980). Forty carefully selected whole-rock samples were analysed for major and trace elements (O'Reilly and Griffin 1988) and over thirty for Sr and Nd isotopes (Griffin et al. 1988). These studies demonstrated that the trace-element patterns of these variably metasomatized mantle rocks reflect the abundance of both primary and metasomatic phases (clinopyroxene, amphibole, mica, apatite). This relationship was explained in terms of open-system crystallization. During metasomatism, the modal composition of the rock determines the bulk partitioning of elements between rock and fluid. If no volatile-bearing phases form, the uptake of LIL and HFS elements is limited essentially by the capacity of clinopyroxene to accept these elements. The variable distribution of metasomatic phases in space and time results in the observed decoupling of major, minor and trace elements during metasomatism.

However, there is still controversy over the true residence sites of the LIL and HFS elements in depleted and metasomatized mantle xenoliths. Many studies, beginning with Griffin and Murthy (1968, 1969) have demonstrated that significant proportions of the LIL elements, in particular, can be removed from some xenoliths by mild acid leaching, and have concluded that large amounts of such elements reside in grain-boundary phases (e.g. Stosch and Lugmair 1986; Zindler and Jagoutz 1988). On the other hand, such acid leaching may also destroy important minor phases and leach material from lattice sites, thus biassing analyses towards artificially depleted compositions.

Several studies of the nature of grain boundaries in mantle-derived xenoliths have used microstructural, microprobe, spectroscopic and scanning techniques. Conclusions range from the interpretation of grain boundaries as refractory regions lacking any low-melting components such as alkalies (e.g. Waff and Holdren 1981)

to their being an important storage site for incompatible elements such as K, Na, P, Ti, Sr, Ba and Ce (e.g. Suzuki 1987).

As a step toward resolving this problem of residence sites, we have determined the trace-element composition of the major and minor phases of twelve well-studied spinel lherzolite xenoliths from the Victorian suite by proton microprobe. This instrument provides precise quantitative analyses of a wide range of trace elements (e.g. Ni, Cu, Zn, Ga, Rb, Sr, Y, Zr, Nb, Ba, Pb, Br and higher levels of the REE, Th and U). This study provides unique data on trace elements directly relevant to mantle metasomatic processes, extending the previously available database restricted to the trace elements measurable by electron and ion microprobe (e.g. Hervig et al. 1986; Bodinier et al. 1987).

The samples include both cryptically and modally metasomatized rocks, and cover the range of trace-element variation observed in the previous studies of this suite (O'Reilly and Griffin 1988). In order to understand both the metasomatic processes and the subsequent nature of potential contamination of basaltic melts by metasomatized mantle, it is important to define: (1) which minerals contain the specific trace elements; (2) the concentrations of these elements. The aims of this work therefore are to characterize the trace-element distribution in metasomatized mantle-wall rock, determine the residence sites of trace elements in metasomatized continental lithosphere, and to quantify effects that were identified qualitatively through whole-rock analysis. From this basis we will also assess how such metasomatized lithosphere may contaminate basaltic melts passing through it.

Methods

Electron-microprobe analyses were carried out on an ETEC Autoprobe at Macquarie University, using methods and standards detailed by Griffin et al. (1984). Whole-rock analyses were carried out by a variety of methods, including XRF, INAA and isotope dilution; the analyses have been presented and discussed in detail by O'Reilly and Griffin (1988).

Most of the samples are too coarse grained (relative to the size of sample available) and too heterogeneous to allow measurement of modal composition by ordinary point-counting. Furthermore, this method would give very imprecise estimates for minor phases such as apatite, which are critical to the trace-element patterns. The modes of the rocks therefore were calculated from the whole-rock composition and electron-microprobe analyses of the constituent minerals, using the least-squares mixing program GENMIX. The trace-element contents of the minerals were then used to calculate the whole-rock contents for comparison with analysed values, and the resulting mass balance used to evaluate the proportion of individual elements that might reside in grain-boundary phases.

Several of the analysed samples contain small amounts of heterogeneous silica-rich glass, produced by partial breakdown of amphibole; textural observations and analyses are given by Griffin et al. (1984). In these samples, the modal calculation typically yielded a negative content for amphibole or clinopyroxene We therefore have not attempted to calculate mass balance for these samples.

An alternative approach (Zindler and Jagoutz 1988) is to crush the rock, separate the phases, and weight the separates. However, this method still leaves the problem of heterogeneity, so that the modally analysed sample may not be representative of the analysed rock. In addition, it risks the preferential loss of some phases to the fine fraction, and is very likely to miss the essential minor phases. Our approach, which takes advantage of the homogeneity of the phases in most of these rocks, assures that the modally and chemically analysed volumes are identical, and avoids the loss of minor phases. Proton-microprobe analyses were carried out at the CSIRO Heavy Ion Analytical Facility, using methods described by Griffin et al. (1988, 1989). A beam of 3 MeV protons is focussed onto the target by an electrostatic lens (Sie and Ryan 1985), forming a spot ca. 20 μm in diameter. The resulting X-rays are collected by a Si(Li) detector, and reduced as discussed in detail by Ryan et al. (1990). In this work the major-element lines were attenuated by a 200-μm Al filter, to allow the use of high beam currents (6–12 nA) and the attainment of low detection limits with reasonable analysis times (3 μC, 5–10 minutes). This choice of filters limits the choice of elements analysed to those with $Z > Fe$. In general, 3–6 spots were analysed on each mineral in a sample; if these appeared to be homogeneous, the spectra of the individual spots were summed to produce a composite spectrum with higher statistics and correspondingly better precision and lower detection limits. Quoted uncertainties are 1 SD, calculated from counting statistics. Minimum detection limits (MDL) are given at the 99% confidence limit, and are considered to be conservative estimates.

The analytical methods employed at HIAF are independent of standards (Ryan et al. 1990), and therefore avoid the problems of standardization associated with ion-microprobe analysis. Analytical data for mafic minerals have been normalized to EMP values for Fe, to correct any bias due to problems in the measurement of accumulated charge. These corrections are typically on the order of 0–10%. Data for apatite are not normalized. Analyses of standard materials (Griffin et al. 1988; Ryan et al. 1990) demonstrate that the accuracy of the method is generally better than 5% relative for concentrations >2–3 x MDL. Comparisons of our data for Sr with isotope dilution (ID) measurements on separated pyroxenes, amphiboles and apatites (see below) confirm this level of accuracy.

Sample descriptions

The modally metasomatized xenoliths from Victoria show a range of microstructures and veining relationships. Isotopic data (Griffin et al. 1988) indicate that there have been at least three distinct metasomatic episodes. The xenoliths chosen for this study represent most of this range as described below. Most commonly, non-composite xenoliths are homogeneous in microstructure, mineral composition (and distribution) and geochemistry on a 20 cm scale (a minimum value limited by xenolith size). The microstructures range from equigranular granoblastic through various degrees of foliation to mylonitic (O'Reilly et al. 1989). These characteristics suggest that processes such as deformation, recrystallization and geochemical re-equilibration have occurred on a scale exceeding 20 cm subsequent to at least some metasomatic events. Some composite xenoliths show geochemical gradients from vein contacts on a cm scale into the mantle wall rock (e.g. Griffin et al. 1984), but some (e.g. WGBM12 of this study) show little detectable change even within 5 cm of the contact. Geochemical gradients in composite xenoliths have been documented from other mantle domains (e.g. northern Queensland, Irving 1980; Dish Hill, California, Nielson et al. 1991).

Modal metasomatism is reflected in the development of volatile-bearing phases such as apatite, amphibole, mica and carbonate, all commonly accompanied by abundant CO_2-rich fluid inclusions (e.g. Andersen et al. 1984). In the Victorian xenoliths, all of these phases may occur discretely or with any combination of the others (although mica has always been found together with amphibole). Modal proportions vary, ranging for example from 10% to <1% for apatite in some lherzolite. Sample BM632 contains a vein 1 cm

wide, consisting of 30% apatite and 70% clinopyroxene. In the western Victoria xenoliths, carbonates occur as tiny crystals projecting from fluid-inclusion walls and are too small for proton-probe analysis. A full description and qualitative analytical data for these carbonates are given in Andersen et al. (1984).

The non-carbonate volatile-bearing minerals may form intrusive veins and networks or they may form an integral part of a granoblastic microstructure. Amphibole commonly appears to have formed at the expense of pre-existing spinel (e.g. O'Reilly 1987) and, more rarely, of clinopyroxene. All diagrams of geochemical data in this paper show the xenoliths in approximate order of increasing degree of metasomatism, taking into account both the modal proportions of volatile-bearing minerals and their general trace-element contents. This order starts with "dry" xenoliths at the left and ranges through those with amphibole, then mica + amphibole, then apatite-bearing assemblages. Calculated modes are given below in Table 7. Samples not listed are either veined, or contain glass, as discussed above.

Results

Typical proton-microprobe spectra for clinopyroxene, amphibole, mica and apatite are shown in Fig. 1; these illustrate the range of elements analysed.

Olivine

Olivine (Table 1) ranges from Fo_{87} to Fo_{91}, averaging Fo_{89}. The only trace elements analysed in all samples are Zn and Ni. Zinc ranges from 37 to 89 ppm, and is roughly correlated with Fe; samples without modal metasomatism tend to have lower Zn for a given Fe content. Nickel ranges from 2,100 ppm to 3,000 ppm (median 2,700), and is roughly correlated with Mg, except for two apatite + amphibole-bearing samples.

Orthopyroxene

Orthopyroxene (Table 2) ranges from En_{87} to En_{91}, averaging $En_{89.7}$. Contents of Al range widely, from the 3–5% typical of opx from spinel lherzolite xenoliths (O'Reilly et al. 1989) to values <1% in several of the most strongly metasomatized samples, which contain spinels with high Cr (Cr + Al), or lack spinel. The TiO_2 content is generally <0.1%, and the higher values are not associated with observable metasomatism. Similarly,

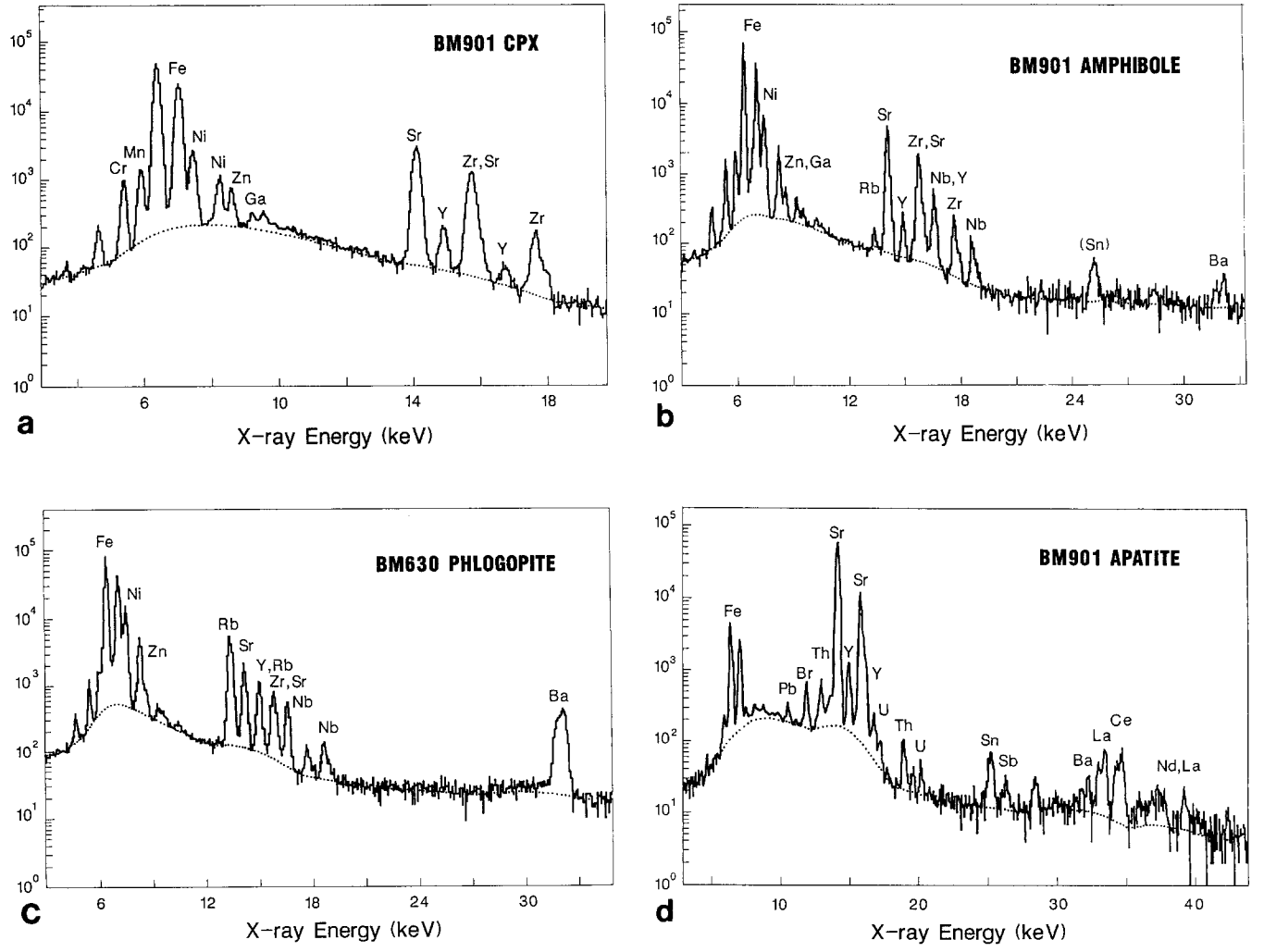

Fig. 1a–d. Representative proton-induced X-ray spectra of metasomatic phases in mantle lherzolites. *Dotted line* is fitted background curve

Table 1. Compositions of olivines

Sample no.	9894	WGBM12	GN23	LE16B	9708	WGBM15	WGBM5	BM630	BM901	BM650	BM655	BM632
Mode[a]	D	D	D	D	(A)	A	A	AM	AAp	AAp	AAp	AAp
SiO_2	40.32	39.80	40.72	40.80	40.89	40.72	40.86	41.42	40.54	40.40	41.29	41.00
FeO	11.42	12.90	10.23	8.75	9.57	11.46	9.52	10.50	12.49	12.12	10.09	9.71
MnO	0.13	0.14	0.14	0.14	0.13	0.15	0.17	0.15	0.18	0.18	0.17	0.14
MgO	48.39	47.20	48.63	50.00	50.21	48.25	49.46	49.80	47.95	47.75	50.06	48.70
CaO						0.06		0.07				
$\sum$	100.26	100.04	99.72	99.69	100.80	100.64	100.01	101.94	101.16	100.45	101.61	99.55
% Fo	88.3	86.7	89.4	91.1	90.3	88.2	90.3	89.4	87.2	87.5	89.8	89.9
ppm												
Ni	2660	2548	836	2940	2790	2640	2730	2950	2100	2630	2720	2480
Zn	52	89	37	46	44	84	55	71	73	116	72	53

[a] *D*, Dry; (*A*), rare amphibole; *A*, common amphibole; *M*, mica; *Ap*, apatite

Table 2. Compositions of orthopyroxenes

Sample no.	9894	WGBM12	GN23	LE16B	9708	WGBM15	WGBM5	BM630	BM901	BM650	BM655	BM632
Mode[a]	D	D	D	D	(A)	A	(A)	AM	AAp	AAp	AAp	AAp
SiO_2	54.55	54.20	56.10	55.20	56.39	56.79	55.13	56.76	56.65	56.90	58.43	57.30
TiO_2	0.17	0.29		0.04			0.16	0.10				
Al_2O_3	5.12	5.06	3.10	3.61	3.08	1.93	4.52	2.50	1.61	0.96	0.73	1.92
Cr_2O_3	0.28	0.39	0.26	0.66	0.35	0.36	0.56	0.48	0.41	0.16	0.21	0.27
FeO	6.97	8.57	6.54	5.61	6.15	7.18	6.06	6.33	7.63	7.55	6.32	6.25
MnO	0.13	0.11	0.15	0.14	0.16	0.17	0.12	0.24	0.20	0.15	0.17	0.18
MgO	32.01	31.60	33.24	33.30	34.18	33.40	32.69	34.14	33.49	33.72	35.22	33.70
CaO	0.83	0.91	0.43	0.89	0.48	0.56	0.85	0.63	0.53	0.53	0.42	0.42
Na_2O	0.12	0.13		0.09		0.07	0.12			0.10	0.06	0.04
$\sum$	100.18	101.26	99.82	99.54	100.79	100.46	100.21	100.96	100.52	100.07	101.56	100.08
% En	89.1	86.8	90.1	91.4	90.8	89.2	90.6	90.6	88.7	88.8	90.9	90.6
ppm												
Ni	773	688	557	799	590	688	717	1660	580		604	
Zn	33	61	13	32	28	58	35	38	57		53	
Ga	2	7	2	2	3	5	3	< 1	3		2	
Sr	2		< 1	2	1	< 1	2	5	< 2		3	
Y	1		< 1	1	< 1	1	2	1	< 1		1	
Zr	4	7	2	2	2	6	5	7	2		6	

[a] As for Table 1

Na_2O contents are not correlated with the presence or absence of volatile-bearing phases. Values of Ni show a narrow range, with a median value of ca. 650 ppm. The range for Zn is generally 30–60 ppm, and is roughly correlated with Fe, as it is in olivine. Most orthopyroxenes contain measurable Ga, but Sr and Y are typically near or below the MDL of 1 ppm. Contents of Zr range 2–7 ppm, but do not seem to be correlated with the degree of metasomatism.

Spinel

Spinels (Table 3) range considerably in both Mg/(Mg+Fe) and Cr/(Cr+Al). These two parameters are poorly correlated, in contrast to the pattern predicated by models of anatexis and melt extraction. The most Cr-rich spinels are found in the most strongly metasomatized rocks; this feature is clearly related to the reaction of spinel+pyroxene+fluid to form amphibole and a more refractory spinel (Griffin et al. 1984; O'Reilly 1987). Contents of Ni are typically 2,000–3,000 ppm, but are lower in the more strongly metasomatized rocks and the veined xenolith GN23. The Zn contents vary widely, and are well correlated with Fe except for sample 9708, which has anomalously high Zn by a factor of two. The Ga contents show a relatively narrow range, and are not correlated with Al content (cf. McKay and Mitchell 1988).

Table 3. Compositions of spinels

Sample no:	9894	WGBM12	GN23	LE16B	9708	WGBM5	BM901	BM655
Mode[a]	D	D	D	D	(A)	(A)	AAp	AAp
TiO_2	0.15			0.20		0.24	0.21	0.11
Al_2O_3	60.01	49.00	51.84	40.70	52.86	51.11	31.27	18.87
Cr_2O_3	7.05	15.20	17.85	27.20	17.10	16.05	35.52	50.80
FeO	11.29	16.90	12.51	13.10	10.91	12.82	19.34	19.92
MnO	0.10	0.20	0.17	0.26	0.18	0.13	0.35	0.48
MgO	20.80	18.10	18.65	18.70	19.48	19.87	14.00	12.27
$\sum$	99.40	99.40	101.02	100.16	100.53	100.22	100.69	102.45
Mg/(Mg+Fe)	76.7	65.6	72.7	71.8	76.1	73.4	56.3	52.3
Cr/(Cr+Al)	7.0	16.5	18.0	29.9	17.1	16.7	42.0	53.2
ppm								
Ni	2760	2560	4206	2020	2222	2560	1030	812
Zn	611	1090	557	695	1200	795	1430	1960
Ga	61	121	66	44	54	65	101	63
Ge	< 2	< 3	< 2	< 2	< 2	< 13	< 5	< 5

[a] As for Table 1

Clinopyroxene

Cpx (Table 4) shows a relatively narrow range of mg [Mg/(Mg+Fe)] and Wo contents, but a wide range in the contents of several minor and trace elements. The highest Al contents are found in the least metasomatized samples, such as 9894 and WGBM12, and the lowest in some of the most strongly metasomatized samples; other samples tend to have ca. 4–5% Al_2O_3. However, other elements commonly ascribed to metasomatic en-

Table 4. Compositions of clinopyroxenes

Sample no:	9894	WGBM12[b]	WGBM12[c]	WGBM12[d]	GN23	LE16B
Mode[a]	D	D	D	D	D	D
SiO_2	51.28	50.10	51.15	50.78	52.81	52.00
TiO_2	0.80	1.02	0.92	1.01	0.21	0.25
Al_2O_3	7.50	7.26	6.40	7.07	4.77	4.65
Cr_2O_3	0.53	0.66	1.13	0.92	0.76	1.22
FeO	3.24	4.30	4.27	4.04	2.44	2.68
MnO	0.11	0.11			0.05	0.08
MgO	15.17	14.90	15.07	14.81	15.54	16.50
CaO	19.30	19.40	19.24	19.35	22.43	21.40
Na_2O	1.90	1.81	1.87	1.71	1.25	1.22
$\sum$	99.83	99.56	100.04	99.68	100.26	100.00
Mg/(Mg+Fe)	89.3	86.1	86.3	86.7	91.9	91.6
ppm						
Ni	320 ±33	302 ±31	309 ±32	326±34	317±33	381 ±40
Cu	< 2	< 3	< 2	3± 0.5	9± 1	< 3
Zn	9 ± 1	22 ± 2	21 ± 2	18± 1	19± 1	11 ± 1
Ga	7 ± 1	13 ± 2	13 ± 1	8± 0.5	5± 1	4 ± 0.5
Ge	2.3± 0.3	2.5± 1	2.3± 0.3	3± 0.2	3± 0.3	3 ± 0.4
Rb	< 1	< 1	< 1	< 1	< 1	< 1
Rb(ID)	–	–	–	–	–	–
Sr	72 ± 3	142 ± 1	143 ± 6	134± 4	153± 6	291 ±11
Sr(ID)	–		–	–	–	–
Y	18 ± 1	16 ± 1	17 ± 1	15± 0.5	9± 1	8 ± 1
Zr	42 ± 2	89 ± 1	91 ± 3	95± 2	16± 1	25 ± 3
Nb	< 1	< 1	< 1	< 1	< 1	4.5± 0.5
Ba	<19	25 ±21	<20	41±15	<18	<19
Pb	< 2	< 2	< 2	< 2	3± 1	< 2

[a] As for Table 1
[b] Adjacent to vein
[c] 1 cm from vein
[d] 5 cm from vein
ID, isotope dilution values (W.L. Griffin and S.Y. O'Reilly, unpubl. data)

richment, such as Ti and Na, show no correlation with the degree of metasomatism. Nickel varies little around a median value of 320 ppm. Zinc varies from 8–32 ppm, with a median of 12 ppm; Ga is typically 5–6 ppm, and is not correlated with Al content. Some Ge is typically present at levels of 2–3 ppm. Strontium shows a large range, from 70 ppm in the unmetasomatized sample 9894, through 100–300 ppm in the weakly metasomatized samples, to 200–700 ppm in the amphibole+apatite-bearing rocks. Yttrium shows little variation around a median value of 12 ppm; the highest values are found in two amphibole+apatite-bearing rocks, and in the unmetasomatized sample 9894. Zirconium is generally low in cpx from the cryptically metasomatized rocks (16–77 ppm) and higher in the more strongly metasomatized rocks. The highest values are found in cpx from some amphibole-rich apatite-free xenoliths. Niobium is at or below MDL in all but ony cpx. Barium is below MDL in all pyroxenes except those coexisting with apatite, where it reaches 50 ppm.

In WGBM12, clinopyroxenes were analysed in the pyroxenite vein, and in the lherzolite at distances of 0–5 cm from the contact. Levels of Cr and Ni are lower, and Fe, Zn and Ga higher, within one cm of the contact. The Sr shows a slight decrease, from 145 to 135 ppm, away from the contact, while Y and Zr show no significant variation.

Amphibole

Amphiboles (Table 5) are essentially titanian chromian pargasites; there is no clear difference in major-element composition between those in veins and those in apparent equilibrium with lherzolite phases. The lowest Ti contents are found in the amphiboles of the amphibole+apatite rocks; these tend to have somewhat higher Na contents, but lower K contents than those in the apatite-free rocks. The highest K content is found in amphibole coexisting with phlogopite (BM630). Contents of Ni are relatively constant about a median value of 730 ppm, and Zn values are similarly constant about a median value of 23 ppm. The Ga values range from <3 to 19 ppm, but are not correlated with Al. Most of the amphiboles contain 5–10 ppm Rb. The range for Sr is 100–700 ppm, reaching the highest values in apatite-bearing rocks. Likewise Zr shows a wide range (15–300 ppm), but is highest in amphiboles from apatite-free rocks. Unlike clinopyroxenes, the amphiboles contain significant amounts of Y and Nb, the latter ranging up to 160

9708 (A)	WGBM15 A	WGBM5 (A)	BM630 AM	BM901 AAp	BM650 AAp Ap vein	BM655 AAp	BM632 AAp
53.13	53.88	52.00	52.37	53.46	50.30	55.13	54.60
0.30	0.21	0.68	0.43			0.36	0.08
4.42	4.02	6.71	4.80	4.00	6.46	2.94	2.99
0.88	1.18	0.96	1.38	1.41	3.16	1.23	0.70
2.25	2.92	3.03	2.80	3.18	2.48	2.59	2.23
	0.10		0.16	0.13		0.10	
15.63	15.59	15.30	15.38	15.68	15.05	15.85	15.81
22.10	20.62	19.44	20.12	20.26	20.60	20.56	21.51
1.15	1.57	1.93	1.82	1.94	1.26	1.94	1.53
99.86	100.09	100.05	99.26	100.06	99.67	100.34	99.45
92.5	90.5	90.0	90.7	89.8	91.5	91.6	92.7
269 ±29	313 ±33	327 ±34	334 ±36	282 ±29	211 ±23	351 ±38	245 ±26
< 2	< 2	< 2	< 2	3 ± 1	< 2	< 4	< 2
15 ± 1	14 ± 1	11 ± 1	11 ± 1	32 ± 2	15 ± 1	17 ± 2	8 ± 1
4± 0.5	10 ± 1	5.5± 0.5	6 ± 0.5	7 ± 0.6	4.5± 0.5	7 ± 1	6 ± 0.5
3.2± 0.3	2.2± 0.3	2.4± 0.3	2.3± 0.3	2.7 ± 0.3	2.3± 0.3	2.5± 0.5	2.6± 0.3
< 1	< 1	< 1	< 1	< 1	< 1	< 1	< 1
–	–	0.005	–	0.14	–	–	–
156 ± 6	176 ± 8	168 ± 7	139 ± 5	207 ± 9	361 ±14	538 ±20	665 ±23
–	–	190	–	212	–	–	–
11 ± 1	10 ± 0.5	14 ± 1	10 ± 0.5	13 ± 1	14 ± 1	22 ± 1	20 ± 1
27 ± 2	214 ± 6	41 ± 2	160 ± 6	90 ± 3	44 ± 4	38 ± 5	114 ± 6
< 1	< 1	1 ± 0.4	< 1	< 1	< 1	< 2	< 1
<25	<20	<20	<20	50 ± 8	24 ± 7	46 ±12	<15
5 ± 1	2.5± 0.7	< 2	< 2	3 ± 1	2.4± 0.6	5 ± 2	< 2

[a] As for Table 1
[b] Adjacent to vein
[c] 1 cm from vein
[d] 5 cm from vein
ID, isotope dilution values (W.L. Griffin and S.Y. O'Reilly, unpubl. data)

Table 5. Composition of amphiboles and mica

Sample no:	9708[b]	WGBM15[b]	WGBM5[b]	BM630[b]	BM901[b]	BM650[b]	BM655[b]	BM632[b]	WGBM12[b]	GN23[b]	BM630[c]
Mode[a]	(A)	A	(A)	AM	AAp	AAp	AAp	AAp	Pxite	Pxite	AM
SiO_2	43.54	43.98	43.17	42.82	44.26	45.17	46.32	45.70	41.90	45.82	38.01
TiO_2	1.54	1.60	3.09	2.93	0.99	0.53	0.40	0.58	4.04	0.92	4.61
Al_2O_3	15.17	13.26	14.55	13.59	13.50	13.18	11.94	12.09	14.93	16.43	16.57
Cr_2O_3	1.17	1.91	1.48	.193	2.13	1.42	2.12	1.33	0.13	0.28	1.56
FeO	3.27	4.15	4.19	3.81	4.37	4.24	3.48	3.31	6.07	3.93	4.00
MnO	0.06	0.07	0.08					0.06			0.07
MgO	18.26	17.32	17.19	16.63	17.75	18.18	18.82	18.49	15.80	17.36	20.49
CaO	11.51	10.95	10.53	10.84	10.53	10.19	10.29	11.00	11.06	11.49	
Na_2O	3.57	3.11	3.17	3.10	3.56	3.91	4.08	3.80	2.83	3.44	0.84
K_2O	0.20	1.28	1.32	1.59	1.09	0.93	0.72	0.64	1.95	0.50	9.46
$\sum$	98.29	97.63	98.77	97.24	98.18	97.75	98.23	96.94	98.78	100.17	95.54
mg	90.9	88.1	88.0	88.6	87.9	88.4	90.6	90.9	82.3	88.7	90.1
ppm											
Ni	632±67	793±84	826±87	729±79	726 ±76	757±81	775 ±82	651 ±69	653 ±68	898 ±93	1320±35
Cu	<6	<3	<4	<4	2.7	<3	44 ± 1	<2	<3	12 ± 1	<2
Zn	24± 3	23± 2	19± 2	20± 2	26 ± 2	34± 3	22 ± 2	14 ± 1	32 ± 2	10 ± 1	24± 1
Ga	< 3	19± 1	7± 1	14± 1	14 ± 1	13± 1	10 ± 1	9 ± 1	17 ± 1	6 ± 1	8± 1
Ge	< 2	<1	2± 0.5	<2	1.5± 0.3	2± 0.5	1.4± 0.4	1.3± 0.3	2.3± 0.4	1.7± 0.4	<1
Rb	< 2	10± 1	13± 1	12± 1	5 ± 1	9± 1	5.5± 0.6	5 ± 0.4	23 ± 2	6 ± 1	282± 9
Sr	105± 6	339±14	555±22	419±17	367 ±14	579±21	709 ±27	796 ±26	534 ±20	307 ±12	127± 4
Sr (ID)	—	—	—	—	373	—	—	—	—	—	—
Y	7± 1	14± 1	15± 1	15±1	17 ± 1	20± 2	21 ± 1	20 ± 1	16 ± 1	17 ± 1	<1
Zr	15± 4	297±10	45± 5	235± 8	132 ± 5	109± 7	64 ± 6	189 ± 8	85 ± 7	38 ± 3	31± 2
Nb	3± 1	65± 2	72± 2	112± 3	67 ± 3	38± 1	7 ± 1	158 ± 4	46 ± 2	68 ± 3	58± 1
Ba	162±28	89±13	442±34	302±20	144 ±18	219±23	307 ±20	462 ±15	296 ±17	215 ±18	2620±63
Pb	< 4	<3	<3	<3	3 ± 1	4± 1	4.6± 0.6	2 ± 0.5	<2	3 ± 1	3± 1
Sn	<11	9± 3	19± 4	16± 4	60 ± 4	<9	<7	9 ± 3	10 ± 2	10 ± 3	

[a] As for Table 1
[b] amphiboles; [c] mica
ID, isotope dilution values (W.L. Griffin and S.Y. O'Reilly, unpubl. data)

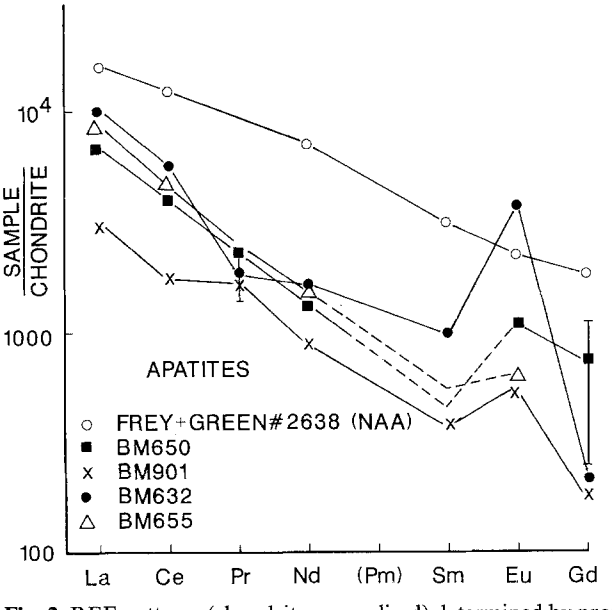

Fig. 2. REE patterns (chondrite-normalised) determined by proton-microprobe analysis for apatites from four metasomatized xenoliths. REE pattern (determined by neutron activation analysis) of apatite from a xenolith described by Frey and Green (1974) is shown for comparison

ppm in one amphibole coexisting with apatite. Barium is also abundant, ranging from 90 to 460 ppm.

Mica

Only one mica was analysed (BM630). It is a titanian phlogopite. Like the amphiboles, it contains significant amounts of Rb, Sr, Nb, and Ba, but is low in Ga and Zr.

Apatite

The apatites (Table 6) are an unusual variety with high contents of CO_2, Cl and OH, but little F (O'Reilly 1987; O'Reilly and Griffin 1988). The significant CO_2 content gives them an unusual appearance in thin section, with first-order interference colours and commonly a dark cloudy texture; they may have been overlooked in many previous studies. They also contain significant amounts of Si, Al, Fe, Mg and Na. Strontium is a significant minor element, reaching more than 2% in some apatites. The apatites also contain a number of other trace elements, including Cu, Zn, Br, Pb, Rb and Zr, at levels of tens of ppm. Thorium U, Y and Ba are present at

Table 6. Compositions of apatites

Sample no:	BM901	BM650	BM655	BM632
Mode[a]	AAp	AAp	AAp	AAp (vein)
SiO_2	0.27	0.54	0.12	0.68
Al_2O_3		1.01	0.06	0.30
FeO	0.47	0.95	0.32	0.49
MgO	1.18		0.83	0.70
CaO	53.09	50.19	50.32	50.4
Na_2O	0.92	0.90	0.96	0.97
P_2O_5	41.72	39.90	38.43	40.0
F	0.26	0.00	0.23	0.15
Cl	1.46	1.67	2.48	2.34
H_2O	0.85	n.a.	n.a.	0.34
CO_2	1.74	n.a.	n.a.	0.66
$\sum$	101.96	95.16	93.75	97.03
ppm				
Ni	< 6	14± 4	< 6	< 11
Cu	17 ± 2	18± 2	22± 2	26±3
Zn	10 ± 1	11± 1	9± 1	6±1
Ga	3.7± 0.6	< 2	< 2	< 3
Ge	3.1± 0.6	3± 1	3± 1	< 3
Br	36 ± 1	22± 1	12± 1	14±1
Rb	< 2	11± 2	21± 1	19±2
Rb(ID)	0.06	–	–	–
Sr	6150 ±146	12200±323	18400±424	23200±610
Sr(ID)	5970	–	–	–
Y	134 ± 3	177± 6	196± 4	245± 8
Zr	23 ± 16	51± 32	26± 29	76± 82
Nb	< 2	< 4	< 3	< 5
Ba	159 ± 21	102± 18	151± 23	359± 26
La	792 ± 46	1740± 59	2140± 85	2510± 67
Ce	1130 ±120	2590±140	2980±122	3620±120
Pr	172 ± 30	219± 37	240± 28	179± 28
Nd	419 ± 52	622± 64	723± 57	823± 78
Sm	<100	< 134	< 164	152± 69
Eu	<130	< 179	< 133	219± 70
Gd	<171	< 216	< 182	< 193
Pb	16 ± 4	30± 4	66± 4	47± 5
Th	150 ± 6	310± 12	673± 26	387± 19
U	70 ± 5	150± 21	249± 15	225± 38

[a] As for Table 1
ID, isotope dilution values (W.L. Griffin and S.Y. O'Reilly, unpubl. data)

100–300 ppm levels. The apatites are extremely light rare-earth-element (LREE) enriched (Fig. 2). Their chondrite-normalized REE patterns are similar to an apatite separated from a Victorian xenolith by Frey and Green (1974), but with somewhat greater LREE enrichment and significant positive Eu anomalies.

Discussion

Trace element residence

The proportional distribution of each element among the phases, calculated from the modes in Table 7, is shown for three typical rocks in Fig. 3. In all three rocks, Ni and Zn reside mainly in olivine, though spinel is an important site for Zn as well. The Ga resides mainly in spinel in the cryptically metasomatized dry rock (LE16B), but this site becomes progressively less important as amphibole becomes more abundant. Strontium, Y and Zr reside almost entirely in the clinopyroxene in the dry rock, but amphibole is an important site in the amphibole-bearing WGBM5 and is the dominant site in the apatite+amphibole-bearing BM901. Apatite, though only making up 1% of the rock, contains ca. 40% of the Sr and 20% of the Y in BM901. The Nb resides entirely in the amphibole, and is below detection in the whole-rock analysis of LE16B.

Figure 4 summarizes the data on the concentration of different trace elements in individual phases; in each diagram the rocks are ranked in order of increasing degree of metasomatism and the histograms are cumulative abundances of the trace elements analysed in the different lherzolite minerals.

The behaviour of compatible elements such as Ni, Zn and Ga appears to be unrelated to the degree of metasomatism. The Ni and Zn contents of olivine, orthopyroxene, clinopyroxene and spinel show little varia-

Table 7. Calculated modes and calculated and analysed trace element whole-rock abundances

Modes	Olivine	Ortho-pyroxene	Spinel	Clino-pyroxene	Amphi-bole	Mica	Apatite	Residuals
9894	44.7	29.8	2.6	23.0	–	–	–	0.18
WGBM12	66.3	24.5	1.2	8.0	–	–	–	0.42
LE16B	77.1	17.7	1.2	4.0	–	–	–	0.20
9708	66.1	21.0	1.5	9.7	1.8	–	–	0.07
WGBM15	69.5	17.6	–	2.6	10.3	–	–	0.13
BM901	62.8	14.6	0.7	8.6	12.7	–	0.6	0.36
BM655	68.4	14.9	0.1	2.8	13.0	–	0.9	0.10

Composition		Ni	Zn	Ga	Sr	Y	Zr	Nb
9894	calculated	1566	51.1	3.8	17.2	4.5	10.9	<1
	analysed	1720	55	3	20.2	8	14	1
WGBM12	calculated	1759	85.4	3	11	1	9.4	<1
	analysed	2269	95	3	11	1	11	1
LE16B	calculated	2448	50.6	1.1	12	0.5	1.4	1.4
	analysed	2644	53	1	12.8	<1	3	<1
9708	calculated	2034	54.3	1.8	17.3	1.9	4.8	0.1
	analysed	2108	55	3	22.9	2	5	2
WGBM15	calculated	2045	71	2.2	39.5	1.9	37.2	6.7
	analysed	2133	76	6	40	5	37	8
BM901	calculated	1527	70.2	3.5	101.3	4.1	24.9	8.8
	analysed	1833	63	3.9	110	5	31	12
Anal. precision[a]		40	2	1	1–2	1	1–3	1

[a] Analytical precision (1 sd) of whole-rock analysis (O'Reilly and Griffin 1988)

tion, and the variation in the Ga content of spinel is not clearly related to Cr/(Cr+Al), nor to metasomatism. However Ga content of spinel decreases with mg of the coexisting olivine, indicating that Ga is a moderately incompatible element and therefore relatively depleted in more refractory lherzolites as suggested by McDonough (1990).

The Ti content of clinopyroxene is highest in the dry rocks, and tends to be lower in clinopyroxene coexisting with amphibole. The Ti content of amphibole drops off markedly in the more apatite-rich rocks. The same is generally true of Nb in amphibole, with the notable exception of sample BM632, where the cpx-apatite vein is bordered by minor amphibole. The Zr contents of both clinopyroxene and amphibole are highest in rocks with these two phases, and lower in the apatite-rich rocks. Barium occurs at significant levels in amphibole, apatite and especially in mica. Clinopyroxene is the main site of Sr, Y and Zr in rocks without volatile phases; in the modally metasomatized rocks, amphiboles become an important site for these elements. The Sr content of both amphibole and cpx increases markedly in the apatite-bearing rocks, while Y increases only slightly.

These figures emphasize the importance of apatite as a site for Sr and Y, as well as the LREE, U and Th, in metasomatized mantle rocks. Sr and Y concentrations increase dramatically with the presence of apatite (note that Fig. 4e shows Sr/100, not Sr). They also demonstrate the importance of amphibole and mica as sites for Ti, Zr, Y, Sr, Ba and Nb (and by inference, for Ta) in the mantle. In particular Nb, essentially is restricted to rocks containing amphibole and mica (Fig. 4g).

Mass balance

Figure 5 summarizes the ranges of several elements in the important carrier phases. For each of these elements, olivine, opx and spinel represent diluents; the figure shows that mass balance is at least theoretically possible, given the right mix of these phases. The calculated modes, and mass-balance calculations based on them, are shown for glass-free rocks in Table 7. These calculations suggest that the trace-element contents of these rocks can be explained, within the analytical and calculation errors, by the trace-element contents of the major and minor phases.

Nickel is consistently underestimated by the modal calculation; the reason for this is not known, but a small error in the calculated olivine/opx ratio would produce a large discrepancy in the calculated Ni. Similarly, a

small error in the apatite/cpx or amphibole/cpx ratios will have strong effects on the calculated contents of Sr, Y and Zr. Nevertheless, the calculations suggest that even in a relatively depleted rock such as WGBM12 or LE16B, less than 20% of the Sr in the rock can reside in grain-boundary phases or other contaminants such as fluid inclusions.

Discussions of the trace-element patterns of depleted and metasomatized mantle xenoliths are plagued by controversy over the true residence sites of the elements in question. As originally shown by Griffin and Murthy (1968, 1969), significant proportions of the LIL elements, in particular, can be removed from some xenoliths by mild acid leaching. Later studies, using very careful handpicking of separated minerals followed by extremely severe leaching, have concluded that the bulk of such elements resides in grain-boundary phases (for example, Zindler and Jagoutz 1988). However, such techniques are not appropriate for the study of metasomatized xenoliths, because many contain trace amounts of apatite, which is difficult to identify and easy to leach out. Furthermore, phases such as mica and amphibole may lose significant quantities of LIL elements during mild leaching (O'Reilly and Griffin 1988).

These reservations may apply also to the study of xenoliths lacking obvious modal metasomatism. Small amounts of volatile-bearing phases may be overlooked and removed during handpicking, or destroyed by extreme acid leaching, and LIL elements may be removed from cryptically metasomatized clinopyroxenes as well by severe leaching. This will lead to estimates of mantle compositions, such as the "clean bulks" of Zindler and Jagoutz (1988), which may be artifically depleted relative to real mantle rocks.

Distribution coefficients

Distribution coefficients and temperature (T) calculated with two-pyroxene thermometers are given in Table 8. The Wood and Banno (1973) thermometer was shown by Griffin et al. (1984) to give temperatures consistent with garnet-clinopyroxene temperatures in composite spinel lherzolite-garnet websterite xenoliths. These values are consistently 50–150° C above temperatures calculated by the thermometer of Köhler and Brey (1990). By either thermometer, these xenoliths represent a restricted range of T, ca. 150–210° C. This is reflected in the generally small range in each distribution coefficient across the sample suite.

The only value that seems to show any temperature variation is the distribution coefficient for Sr between clinopyroxene (cpx) and orthopyroxene (opx), which becomes smaller at higher temperatures. This reflects the extremely low Sr contents of the lower-T orthopyroxenes. Zindler and Jagoutz (1988) report values for K_D^{Sr} (cpx/opx) of 323–413, about twice our highest value. This may suggest that extreme acid leaching has depleted their pyroxenes, and preferentially the orthopyroxene, in Sr. Our analytical values for Sr in opx are near the MDL, and should be treated with caution; however,

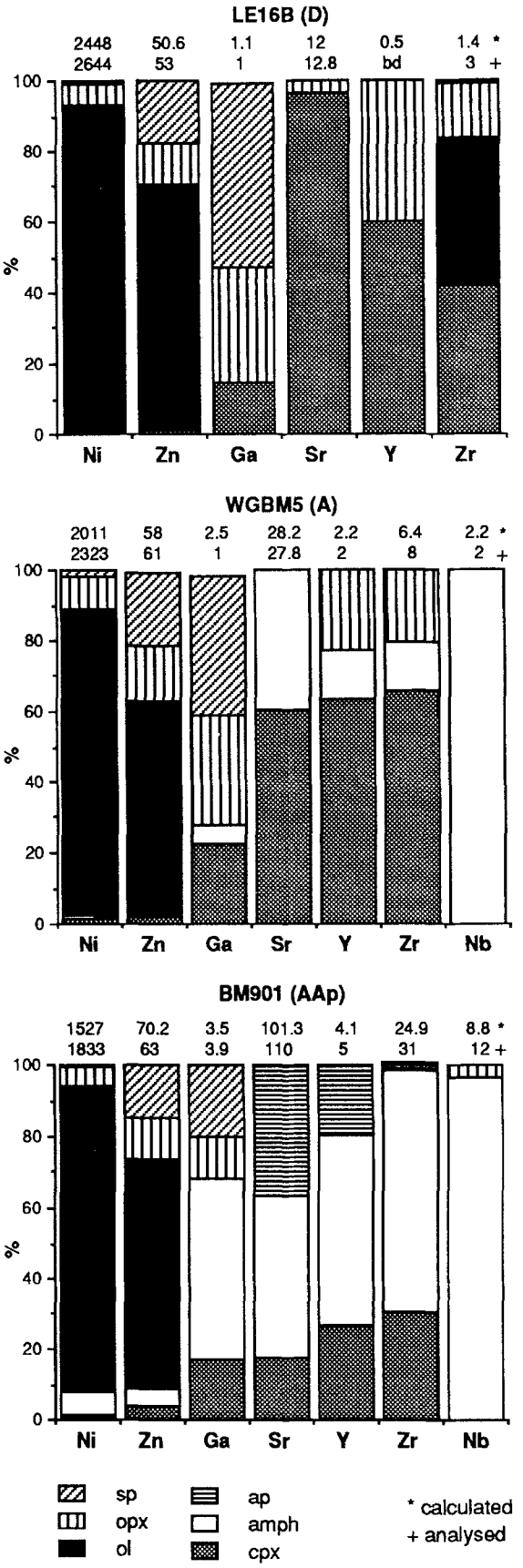

Fig. 3. Relative proportions of selected trace elements in individual phases of three lherzolites, representing varying degrees of metasomatism: *D*, dry; *A*, amphibole present; *AAp*, amphibole and apatite present. Analysed and calculated whole-rock abundances are shown at the top of each column

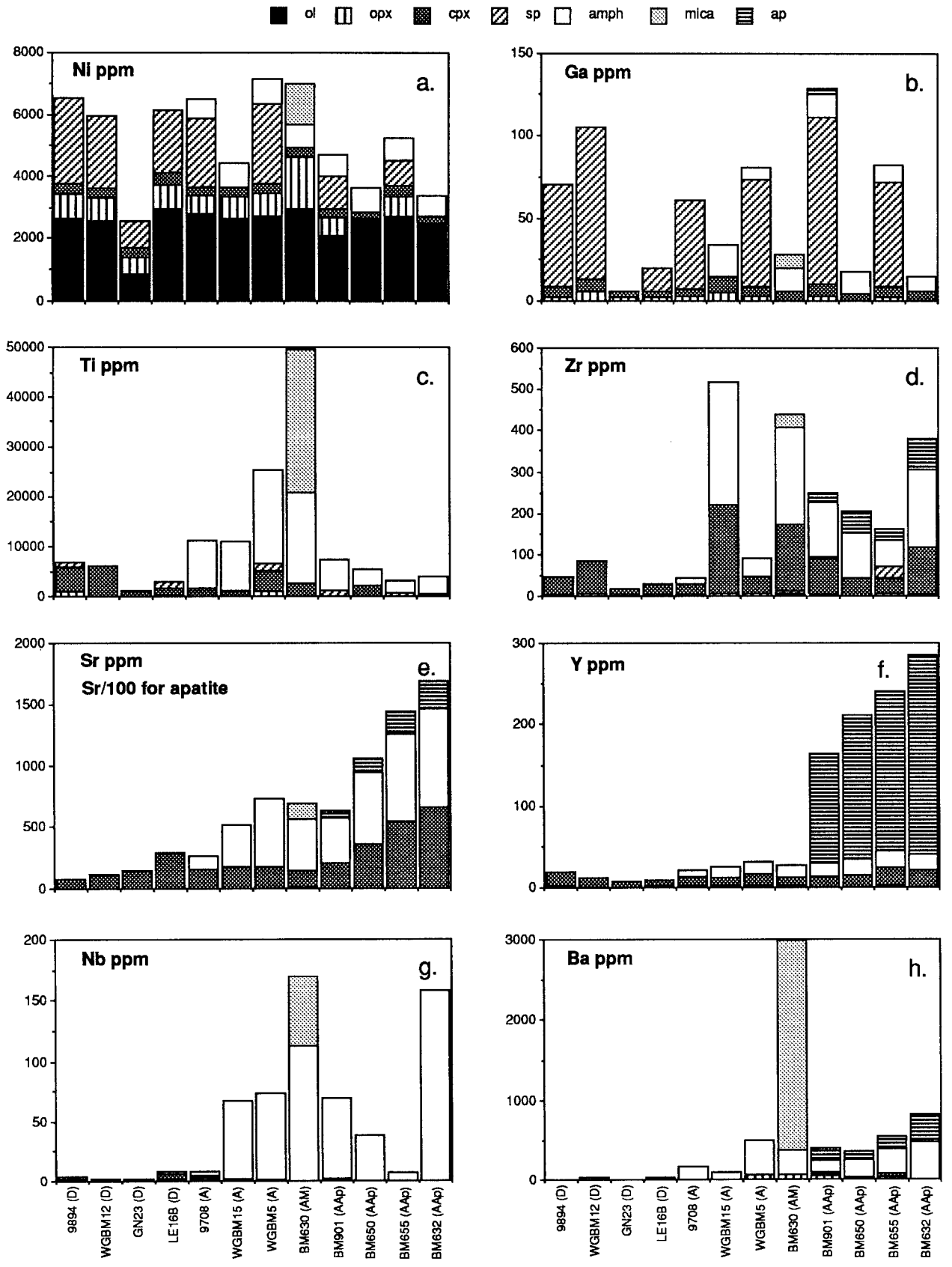

Fig. 4a–h. Cumulative absolute abundances of selected trace elements in particular minerals in the lherzolites. Rock samples are arranged in inferred order of increasing metasomatism: dry rocks are plotted at *left* followed by those carrying amphibole, then amphibole + mica, with apatite-bearing ones on the *right*. See text for discussion

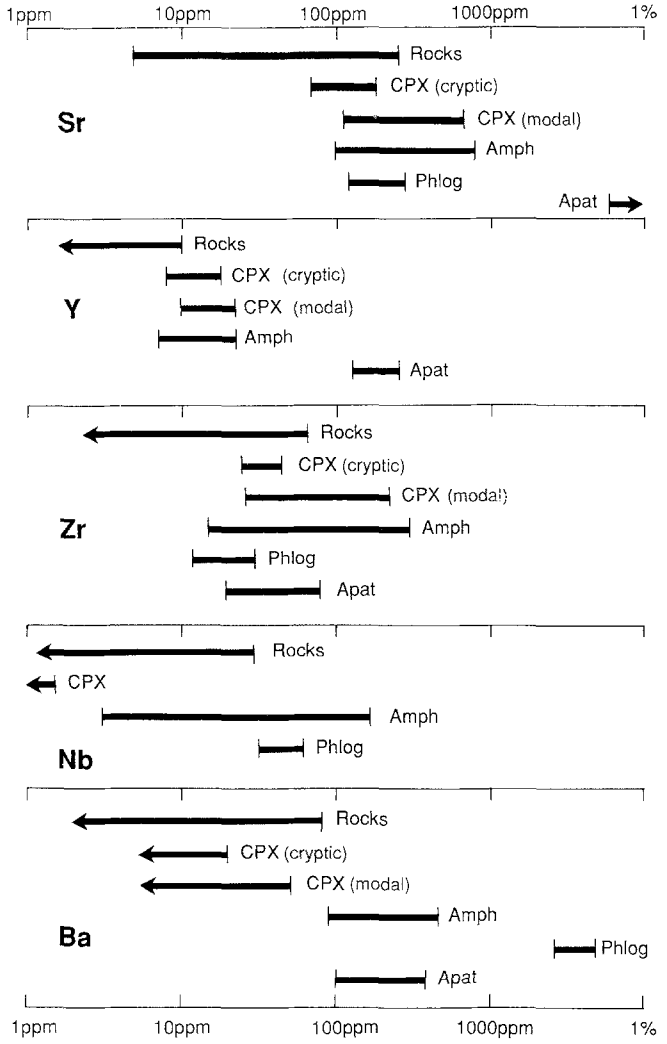

Fig. 5. Summary of the ranges and abundances (note log scale) of Sr, Y, Zr, Nb and Ba in clinopyroxenes (for both cryptically and modally metasomatized rocks), amphibole, phlogopite and apatite

we regard the higher values as significant, and they are roughly ten times the levels reported by Zindler and Jagoutz.

The general uniformity of the individual distribution coefficients across the sample suite suggests that they may be used to test for equilibrium among the metasomatic phases. Apatite/cpx coefficients are very constant, except for the anomalous values for Zn and Zr in BM901. Apatite/amphibole coefficients are also relatively constant, except for the unusual values for Sr, Zr and Ba in BM901. Amphibole/cpx coefficients show even less variation, with the exception of 9708, which is anomalous in Ga, Sr, Y and Zr.

These data suggest that amphibole, apatite and clinopyroxene are in equilibrium in most samples, but not in all. In BM901, clinopyroxene and amphibole appear to be in mutual equilibrium, but apatite may not be in equilibrium with either. This is consistent with isotopic evidence; the amphibole and cpx have identical $^{87}Sr/^{86}Sr$ (0.70502 ± 3) and $^{143}Nd/^{144}Nd$ (0.51268 ± 1), but the apatite is slightly different (0.70495 ± 1, 0.51264 ± 1). Since the apatite has lower Rb/Sr and Sm/Nd than the other phases, these differences might reflect isotopic evolution over time; however, the three phases do not define an isochron. We interpret the combined trace-element and isotopic disequilibrium as suggesting the apatite was introduced in an event separate from the formation of amphibole and mica, as originally suggested on isotopic grounds by Griffin et al. (1988).

Metasomatism near mafic veins

WGBM12 is a composite xenolith, showing contact between anhydrous spinel lherzolite and a clinopyroxene-amphibole vein. O'Reilly and Griffin (1988) proposed that such veins represent the products of crystallizing mafic melts, and that they are the immediate source of fluids responsible for metasomatism of the lherzolite wall rocks.

The trace-element content of clinopyroxene near the pyroxenite/lherzolite contact in WGBM12 is very similar to that of pyroxene in the vein. The Sr content of the clinopyroxene drops slightly over a distance of 5 cm from the contact, while Y and Zr contents are essentially constant. The pyroxene 5 cm from the contact is still enriched in Sr and Zr relative to the pyroxene of an unmetasomatized xenolith such as 9894 (Fig. 4). We infer that Sr, Y and Zr were introduced by fluids moving away from the vein, and that gradients in these elements probably extended beyond the 5 cm that could be sampled in this xenolith. These data suggest that the effects of cryptic metasomatism of clinopyroxene diminish over distances of cm to dm away from the source of the metasomatizing fluids, and that gradients of Zr and Y extend further than that of Sr. This is consistent with the arguments of Navon and Stolper (1987), who propose that more compatible elements will be removed more quickly from an infiltrating fluid, with the wall rock acting as a chromatographic column. In this case, elements relatively compatible with clinopyroxene, such as Sr and Zr, are concentrated in clinopyroxene near the vein, and removed from the fluid. Other elements, such as U, Th, Rb, Ba and LREE, which are less compatible in cpx, probably penetrated farther into the rock.

If the lherzolite wall rock acts as a chromatographic column in this way, it is unlikely that the observed metasomatism of the spinel lherzolite xenoliths in the Victorian suite has been caused by long-distance percolation of fluids through the mantle. A more likely model involves the expulsion of fluids from a network of veins, filled with crystallizing basic melts (Wilshire 1987; Andersen et al. 1984; Navon and Stolper 1987; O'Reilly and Griffin 1988; Nielson et al. 1991). That Ni, Zn and Ga are not introduced by the percolating fluid responsible for the metasomatism suggests that the fluid is not a conventional silicate mantle melt. In addition, the precipitation of apatite rich in Cl and CO_2 provides strong evidence that this apatite forming fluid is carbonate-rich.

The data presented here, combined with the models for Navon and Stolper (1987) illustrate the crucial role of crystal chemistry in determining the effects of metaso-

Table 8. Calculated temperatures and distribution coefficients

	T °C			K_d^d							
	BKN[a]	WB[b]	SS[c]	Ni	Zn	Ga	Sr	Y	Zr	Nb	Ba
Clinopyroxene/orthopyroxene											
9894	1036	1087	1048	0.41	0.27	3.5	36	18	11	–	–
WGBM12	1003	1082	1130	0.44	0.31	1.2	>112	>12	10	–	–
LE16B	930	1078	1029	0.48	0.34	2	145	8	13	–	–
9708	841	992	1029	0.45	0.54	1.3	156	>11	14	–	–
WGBM15	955	1022	–	–	–	–	–	–	–	–	–
WGBM5	1036	1089	1052	0.45	0.31	1.8	84	7	8	–	–
BM630	946	1035	–	0.2	0.29	>6	28	10	*23*	–	–
BM901	909	1013	840	0.49	0.56	2.3	>103	>13	*45*	–	–
BM655	904	998	791	0.58	0.32	3.5	179	22	6	–	–
GN23	741	940	890	0.62	*1.8*	2	>145	> 8	9	–	–
Spinel/clinopyroxene											
9894	1036	1087	1048	8.6	68	8.7	–	–	–	–	–
WGBM12	1003	1082	1130	7.2	55	13	–	–	–	–	–
LE16B	930	1078	1029	5.3	63	11	–	–	0.07	0.44	–
9708	841	992	1029	8.3	80	13.5	–	–	–	–	–
WGBM15	955	1022	–	–	–	–	–	–	–	–	–
WGBM5	1036	1089	1052	7.8	72	11.8	–	–	–	–	–
BM630	946	1035	–	–	–	–	–	–	–	–	–
BM901	909	1013	840	3.7	45	14.4	–	–	–	–	–
BM655	904	998	791	2.3	*115*	9	–	–	–	–	–
GN23(diseq)	741	940	890	2.4	1.5	1	–	–	–	–	–
Amphibole/clinopyroxene											
9708	841	992	1029	2.3	1.6	*<0.8*	*0.67*	*0.64*	*0.56*	–	–
WGBM15	955	1022	–	2.5	1.6	1.9	1.9	1.4	1.4	–	–
WGBM5	1036	1089	1052	2.5	1.7	1.3	*3.3*	1.1	1.1	–	–
BM630	946	1035	–	2.2	1.8	2.3	*3*	1.5	1.5	–	–
BM901	909	1013	840	2.6	0.8	2	1.8	1.3	1.5	–	–
BM655	904	998	791	2.2	1.3	1.4	1.3	1	1.7	–	–
BM632	825	952	–	2.7	1.8	1.5	1.2	1	1.7	–	–
BM650	980	1049	–	3.6	2.3	2.9	1.6	1.4	2.5	–	–
Amphibole/mica											
BM630	946	1035	–	0.55	0.83	1.8	1.9	>15	7.6	1.9	0.12
Apatite/clinopyroxene											
BM901	909	1013	840	–	*0.31*	–	30	10	*0.26*	–	–
BM655	904	998	791	–	0.53	–	34	9	0.68	–	–
BM632	825	952	–	–	0.75	–	35	12	0.67	–	–
BM650	980	1049	–	0.06	0.73	–	34	13	1.2	–	–
Apatite/amphibole											
BM901	909	1013	840	–	0.38	–	*0.26*	17	*0.17*	–	*1.1*
BM655	904	998	791	–	0.41	–	26	9	0.41	–	0.49
BM632	825	952	–	–	0.42	–	29	12	0.40	–	0.78
BM650	980	1049	–	0.02	0.32	–	21	9	0.47	–	0.47

[a] Brey, Köhler and Nickel (1990)
[b] Wood and Banno (1973)
[c] Sachtleben and Seck (1982)
[d] Values in italics are aberrant (see text for discussion)

matic processes in the mantle. Metasomatism is an open-system process, by definition. In an open system, the bulk distribution coefficient between the rock and a percolating fluid will be determined by the mineral assemblage; the modal composition will be especially important where different phases have widely different abilities to accept individual elements.

In the case of anhydrous spinel lherzolite, the ability of the rock to extract Sr, Zr, Y and LREE from the fluid is limited primarily by the cpx/fluid distribution coefficients and the abundance of cpx. However, if amphibole and/or mica are present, or are formed as a consequence of metasomatism, the rock can extract greater amounts of these elements from the fluid. Conversely, the levels of elements such as Rb, Nb, Ta and Ba in the whole rock can be rasied significantly only if these phases are present. The presence of apatite allows more extreme enrichments in Sr, LREE and Y; it also provides sites for U and Th, as well as more exotic elements such as Br.

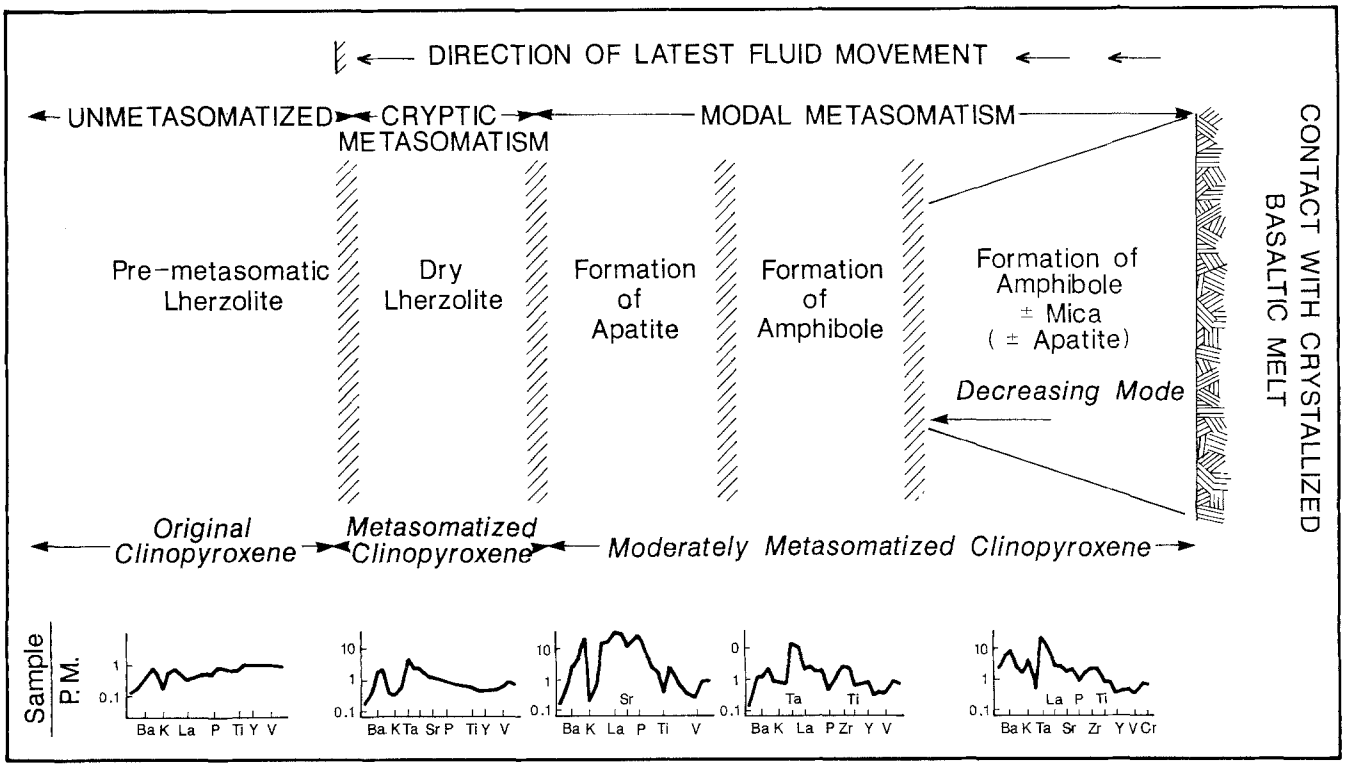

Fig. 6. Cartoon illustrating the formation of successive zones of metasomatism by fluids released from crystallization of silicate melts. Trace-element patterns are median values and are normalised to primordial mantle, *P.M.* All sources are given in O'Reilly and Griffin (1988)

The precipitation of amphibole, mica and apatite is likely to vary widely in space and time throughout a metasomatic episode, depending on *P*, *T* and the details of fluid composition. These variations can lead to marked decoupling of the major- and trace-element effects of metasomatism, and wide variations in the major- and trace-element patterns of the metasomatized lherzolite (Fig. 6). O'Reilly and Griffin (1988) noted that, contrary to common models (Hawkesworth et al. 1984), enrichment of K and Ti does not accompany enrichment in Fe in the Victorian xenolith suite. They ascribed this to local precipitation of mica at vein margins; the mica effectively would remove K and Ti (as well as Rb and Ba) from the fluids and concentrate it in relatively small volumes, while Fe would penetrate further into the rock. Similarly, U, Th and LREE might be expected to penetrate relatively far into the wall rocks, in the absence of apatite. However, once apatite has formed, these elements probably would be quantitatively removed from the fluid. It is noteworthy that the Ti, Zr and Nb contents of clinopyroxene and amphibole are generally lower in apatite-rich rocks than in those with little or no apatite. This is consistent with apatite forming only after these elements have been removed from the percolating fluid by precipitation of amphibole and mica.

The origin of the low-Ti amphiboles in these xenoliths thus can be explained by metasomatic precipitation from a fluid of progressively changing composition. Their origin is distinct from that inferred for low-Ti amphiboles in xenoliths from the Rhenish Massif, which are interpreted as products of reaction between mantle peridotite and a stationary grain-boundary fluid in a rising diapir (Witt and Seck 1989).

Implications for intraplate basalt heterogeneity

Spinel lherzolite mantle wall rock does not represent the source rock for intraplate alkali (and some tholeiite) basalts; basalt REE patterns require residual garnet in the source and experimental results are consistent with partial melting in the garnet lherzolite region (Green and Ringwood 1967). Therefore arguments about the relevance of metasomatized spinel lherzolite to alkali basalt compositions have been based on an assumption that the products and processes in the spinel lherzolite zone reflect those in the deeper source regions. This may well hold true, but there is also an added complexity in that magmas derived at deeper levels must pass through any mantle material in the spinel lherzolite field.

Alkali basaltic magmas show extensive heterogeneity in minor and trace element content both from region to region and within regions (e.g. Wass 1980; O'Reilly and Griffin 1984; Clague and Frey 1982; Frey et al. 1978; Kempton et al. 1987). A common interpretation is that such heterogeneity reflects source characteristics and different degrees of partial melting. However, passage of small-volume primitive or primary melts through metasomatized spinel peridotite enriched in HFS and LIL elements may result in contamination of these melts. This study has shown that the trace elements in modally metasomatized mantle rocks reside in phases such as

amphibole, mica and apatite which are less refractory and easily broken down (e.g. Amundsen 1987) in heating events such as those due to the passage of magma along adjacent conduits or networks. When these phases break down, the trace elements cannot be accepted into the residual lherzolite phases and are therefore partitioned into the melt. This mechanism thus provides very easy contamination of ascending or infiltrating small-volume magmas.

The concept of the mantle as a chromatographic column has been developed by Hofmann (1986) and Navon and Stolper (1987). Hofmann clearly illustrates that with respect to large-volume melts such as the Hawaiian shield tholeiites, such a model presents insurmountable difficulties because of the scale and uniformity of metasomatism required by the uniform but non-primitive Nb/U and Nb/Th ratios of the shield-forming basalts.

However, with small-volume melts (such as those for intraplate alkali basalts), if there is sufficient contact, the melts and wall rocks will interact chemically to an extent determined by the time of exposure. Navon and Stolper's modelling demonstrates that for trace elements, the change in incompatible elements occurs faster than for compatible elements and that extreme fractionations may occur by chromatographic exchange processes. This effect is enhanced when metasomatic phases such as amphibole, mica and/or apatite are present as these phases are less refractory (and thus break down with heating) and also act as reservoirs for LIL and HFS elements.

The bulk trace-element geochemical signature of the metasomatized mantle rocks beneath western Victoria (O'Reilly and Griffin 1988) is very similar to that calculated for the source compositions for alkali basaltic rocks from that region (Frey et al. 1978). It also closely resembles the calculated source for Honolulu volcanics (Clague and Frey 1982) and, analogously, trace-element compositions of spinel lherzolite xenoliths from Salt Lake Crater (Reid and Woods 1978; Frey 1980). These observations suggest that the trace-element signature of the alkali basalt may result largely from interaction with metasomatized spinel lherzolite mantle wall rock.

Therefore, the heterogeneity observed in the trace-element patterns of sequences of continental basaltic rocks does not necessarily reflect source heterogeneity. It may merely be the cumulative imprint of varying degrees of contamination by different types of metasomatized lithospheric mantle. Thus the trace-element signatures of such basalts may carry little information either about their source or about differentiation processes.

Conclusions

Trace element residence and distribution

1. High levels of LIL and HFS elements in spinel lherzolites require modal metasomatism and the availability of specific, metasomatically introduced, acceptor minerals, In particular, high levels of REE, Sr (and U, Th, Br) require apatite, high Ba requires mica and/or amphibole, high Nb and Ta require amphibole or mica.
2. In *cryptic* metasomatism of spinel lherzolite, enrichment in trace elements can occur only up to the levels controlled by the K_D value for clinopyroxene/fluid.
3. The mineral trace-element analyses and mass-balance calculations show good correlations between analysed and calculated trace-element abundances for whole rocks. There is therefore no significant concentration of the analysed trace elements at clean grain boundaries devoid of glass or alteration.
4. K_D values show little variation over the temperature range seen in these rocks. The uniformity of K_Ds established in this study indicates that these can be used to test equilibrium between metasomatic phases and pre-metasomatic phases.

Metasomatic processes and model

1. Metasomatism is a dynamic, open-system process, with introduced trace elements contained in specific minerals. It is essential that studies of metasomatism recognize the importance of crystal-chemical controls, rather than treating rocks as amorphous sponges.
2. The metasomatism observed in the Victorian lherzolites is ascribed to infiltration of fluids released by crystallizing silicate melts (Andersen et al. 1984; O'Reilly and Griffin 1988). These released fluids change composition as different metasomatic minerals form successively during their infiltration through the mantle wall rock. This process produces metasomatic zones with different model mineralogies. Each of these fronts or zones has a specific geochemical signature (Fig. 6) determined by (i) the model proportion of minerals present (in practice, clinopyroxene and those formed in the metasomatic process) and (ii) the crystal/fluid partition coefficients of these minerals.

Consequences for alkali basaltic compositions

1. The trace-element composition of some metasomatized spinel lherzolite mantle domains is compatible with calculated sources for intraplate basanite (e.g. western Victoria (Frey et al. 1978) and the Honolulu volcanics (Clague and Frey 1982)).
2. LIL and HFS elements in metasomatized mantle reside largely in less refractory minerals which will be the first to melt when in contact with magma conduits. Melting or breakdown of acceptor minerals will partition specific trace elements into the melt, resulting in easy and variable contamination of ascending magmas.
3. The trace-element heterogeneity of alkali basaltic rocks may not reflect directly source heterogeneity or differentiation processes but may be largely a result of contamination by metasomatized spinel lherzolite mantle wall rock.

Acknowledgements. We are grateful to Norm Pearson for computing and electron microprobe assistance, and to G Suter and R Mackay for technical assistance on the proton microprobe. The Australian Museum provided some of the samples. Financial support was provided by a CSIRO/Macquarie collaborative grant, ARC grant A33831447, and Stockdale Prospecting Ltd. The origi-

nal draft was improved by the comments of W McDonough, NJ Pearson, HA Seck, H-G Stosch, SS Sun and G Witt.

References

Amundsen HEF (1987) Evidence for liquid immiscibility in the upper mantle. Nature 327:692–695

Andersen T, O'Reilly SY, Griffin WL (1984) The trapped fluid phase in upper mantle xenoliths from Victoria, Australia: implications for mantle metasomatism. Contrib Mineral Petrol 88:72–85

Brey GP, Köhler TP, Nickel KG (1990) Geothermobarometry in natural four-phase lherzolites, part 1: experimental results from 10–60 kbar. J Petrol 31:1313–1352

Bodinier JL, Dupuy C, Dostal J, Berlet C (1987) Distribution of trace transition elements in olivine and pyroxenes from ultramafic xenoliths: application of microprobe analysis. Am Mineral 72:902–913

Clague DA, Frey FA (1982) Petrology and trace element geochemistry of the Honolulu Volcanics, Oahu: implications for the oceanic mantle below Hawaii. J Petrol 23:447–504

Dawson JB (1980) Kimberlites and their xenoliths. Springer-Verlag, New York

Frey FA (1980) The origin of pyroxenites and garnet pyroxenites from Salt Lake Crater, Oahu, Hawaii: trace element evidence. Am J Sci 280-A:427–449

Frey FA, Green DA (1974) The mineralogy, geochemistry and origin of lhezrolite inclusions in Victorian basanites. Geochim Cosmochim Acta 38:1023–1059

Frey FA, Green DA, Roy SD (1978) Integrated models for basalt petrogensis: a study of quartz tholeiites to olivine melilities from south eastern Australia utilizing geochemical and experimental petrological data. J Petrol 19:463–513

Green DA, Ringwood AE (1967) The genesis of basaltic magmas. Contrib Mineral Petrol 5:103–190

Griffin WL, Murthy VR (1968) Abundances of K, Rb, Sr and Ba in some ultramafic rocks and minerals. Earth Planet Sci Lett 4:497–501

Griffin WL, Murthy VR (1969) Distribution of K, Rb, Sr and Ba in some mineral relevant to basalt genesis. Geochim Cosmochim Acta 33:1389–1414

Griffin WL, Wass SY, Hollis JD (1984) Ultramafic xenoliths from Bullenmerri and Gnotuk maars, Victoria, Australia: petrology of a sub-continental crust-mantle transition. J Petrol 25:53–87

Griffin WL, O'Reilly SY, Stabel A (1988) Mantle metasomatism beneath western Victoria, Australia II: isotopic geochemistry of Cr-diopside lherzolites and Al-augite pyroxenites. Am J Sci 280-A52:449–459

Griffin WL, Jaques AL, Sie SH, Ryan CG, Cousens DR, Suter GF (1988) Conditions of diamond growth: a proton microprobe study of inclusions in West Australian diamonds. Contrib Mineral Petrol 99:143–152

Griffin WL, Smith D, Boyd FR, Cousens DR, Ryan CG, Sie SH, Suter GF (1989) Trace element zoning in garnets from sheared mantle xenoliths. Geochim Cosmochim Acta 53:561–567

Hawkesworth CJ, Rogers NW, van Calsteren PWC, Menzies MA (1984) Mantle enrichment processes. Nature 311:331–335

Hervig RL, Smith JV, Dawson JB (1986) Lherzolite xenoliths in kimberlites and basalts: petrogenetic and crystallochemical significance of some minor and trace elements in olivine, pyroxenes, garnet and spinel. Trans R Soc Edinburgh Earth Sci 77:181–201

Hofmann AW (1986) Nb in Hawaiian magmas: constraints on source composition and evolution. Chem Geol 57:17–30

Irving AJ (1980) Petrology and geochemistry of composite ultramafic xenoliths in alkalic basalts and implications for magmatic processes in the mantle. Am J Sci 280-A:389–426

Kempton PP, Dungan WA, Blanchard DP (1987) Petrology and geochemistry of xenolith-bearing alkalic basalts from the Geronimo Volcanic Field, southeast Arizona: evidence for polybaric fractionation and implications for mantle metasomatism. In: Morris EM, Pasteris JD (eds) Mantle metasomatism and alkaline magmatism. Geol Soc Am Spec Pap 215, pp 347–370

Köhler TP, Brey GP (1991) Ca exchange between olivine and clinopyroxene calibrated as a geothermobarometer for natural peridotites from 2 to 60 kbar with applications. Geochim Cosmochim Acta 54:2375–2388

McDonough WF (1990) Comment on "Abundance and distribution of gallium in some spinel and garnet lherzolites" by D.B. McKay and R.H. Mitchell. Geochim Cosmochim Acta 54:471–473

McKay DB, Mitchell RH (1988) Abundance and distribution of gallium in some spinel and garnet lherzolites. Geochim Cosmochim Acta 52:2867–2870

Navon O, Stolper E (1987) Geochemical consequences of melt percolation: The upper mantle as a chromatographic column. J Geology 95:285–307

Nielson JE, Budahn JR, Unruh DM, Wilshire HG (1991) An actualistic model of mantle metasomatism documented in a composite xenolith from Dish Hill, California. Geochim Cosmochim Acta (in press)

O'Reilly SY (1987) Volatile-rich mantle beneath eastern Australia. In: Nixon PH (ed) Mantle xenoliths. Wiley, London, pp 661–670

O'Reilly SY, Griffin WL (1984) Sr isotopic heterogeneity in primitive basaltic rocks, southeastern Australia: correlation with mantle metasomatism. Contrib Mineral Petrol 87:220–230

O'Reilly SY, Griffin WL (1988) Mantle metasomatism beneath Victoria, Australia I: metasomatic processes in Cr-diopside lhzerolites. Geochim Cosmochim Acta 52:433–447

O'Reilly SY, Nicholls IA, Griffin WL (1989) Xenoliths and megacrysts of mantle origin. In: John RW (ed) Intraplate volcanism in Eastern Australia and New Zealand. Cambridge University Press, pp 254–274

Reid JB, Woods GA (1978) Oceanic mantle beneath the southern Rio Grande Rift. Earth Planet Sci Lett 41:254–274

Ryan CG, Cousens DR, Sie SH, Griffin WL, Clayton EJ (1990) Quantitative PIXE microanalysis in the geosciences. Nucl Instrum Methods B47:55–71

Sachtleben T, Seck HA (1982) Chemical control of Al-solubility in orthopyroxene and its implications for pyroxene geothermobarometry. Contrib Mineral Petrol 78:157–165

Sie SH, Ryan CG (1985) An electrostatic "Russian" quadruplet microprobe lens. Nucl Instrum Methods Phys Res B15:664–670

Stosch H-G, Lugmair GW (1986) Trace element and Sr and Nd isotopic geochemistry of peridotite xenoliths from the Eifel (West Germany) and their bearing on the evolution of the subcontinental lithosphere. Earth Planet Sci Lett 80:281–298

Suzuki K (1987) Grain-boundary enrichment of incompatible elements in some mantle peridotites. Chem Geol 63:319–334

Waff HS, Holdren GR (1981) The nature of grain boundaries in dunite and lherzolite mantle xenoliths: implications for magma transport in refractory upper mantle material. J Geophys Res 86:3677–3683

Wass SY (1980) Geochemistry and origin of xenolith-bearing and related alkali basaltic rocks from the Southern Highlands NSW, Australia. Am J Sci, Jackson Vol 280A:639–666

Wilshire HG (1987) A model of mantle metasomatism. In: Morris EM, Pasteris JD (eds) Mantle metasomatism and alkaline magmatism. Geol Soc Am Spec Pap 215, pp 47–60

Witt G, Seck HA (1989) Origin of amphibole in recrystallized and porphyroclastic mantle xenoliths from the Rhenish Massif: implications for the nature of mantle metasomatism. Earth Planet Sci Lett 91:327–340

Wood BJ, Banno S (1973) Garnet-orthopyroxene and orthopyroxene-clinopyroxene relationships in simple and complex systems. Contrib Mineral Petrol 42:109–121

Zindler A, Jagoutz E (1988) Mantle cryptology. Geochim Cosmochim Acta 52:319–333

Editorial responsibility: J. Touret